OPTRONIC™
LABORATORIES

SPECTRAL RESPONSE OF A UV FLAME SENSOR FOR MODERN TURBOJET AIRCRAFT ENGINE

By William E. Schneider and George L. Minott
August 1989

Reprinted from 1989 SPIE San Diego Proceedings

Reprint Number: R05 | Cover Sheet Updated: Mar 2019 | OptronicLabs.com

SPECTRAL RESPONSE OF A UV FLAME SENSOR FOR A MODERN TURBOJET AIRCRAFT ENGINE

by

William E. Schneider
Optronic Laboratories, Inc., Orlando, FL 32811

and

George L. Minott
Armtec Industries, Inc., Manchester, NH 03103

ABSTRACT

One of the military's newest carrier-based attack aircraft is powered by a modern turbojet engine. This turbojet engine provides additional thrust for combat maneuvers and carrier takeoffs from an afterburner (the burning of additional fuel "after the burning" in the main or core engine). To improve reliability of "light-off" characteristics and to provide safeguards against undesired afterburner "light-off" conditions, an ultraviolet flame sensor is employed. The flame sensor contains a UV detector which is a gaseous-discharge-type tube manufactured by Armtec Industries, Inc. In order to better determine the relationship between flame and sensor, measurements of the UV spectral response of the sensors were made at ambient and elevated (400°F) temperatures.

The measurements, which were made by Optronic Laboratories at Armtec's Manchester, New Hampshire facility, utilized a double monochromator-based system optimized for measuring the spectral response of detectors over the 200 to 300 nm wavelength region. The paper describes the UV-flame sensor, the instrumental set-up, the measurement procedure, the NIST-traceable standards and the results and uncertainties associated with the measurements.

1. INTRODUCTION

The GE-manufactured F404 aircraft engine is the powerplant of the U.S. Navy's newest aircraft, the F/A-18 carrier based attack fighter. This turbojet engine provides additional thrust for combat maneuvers and carrier takeoffs from an afterburner (the burning of additional fuel "after the burning" in the main or core engine). To improve the reliability of afterburner "light-off" characteristics and to provide safeguards against undesired afterburner"light-off" conditions, an ultraviolet flame sensor is employed. The flame sensor uses a proprietary solar blind, UV gaseous-discharge-type detector designed and manufactured by Armtec Industries, Inc.

Unstable operation of the afterburner's gas exit nozzle has been a field complaint. This intermittent condition designated as VEN (Variable Exhaust Nozzle) cycling is an undesirable operating condition and was assessed to be associated with a low output signal from certain flame sensor units at elevated temperature.

In normal operation, the flame sensor detects ultraviolet radiation from the engine's afterburner hydrocarbon flame. When this occurs, output voltage pulses are fed from the flame sensor to the engine control unit circuit. There the pulses are integrated into a DC voltage to trigger the control logic which indicates that a "light-off" (ignition of fuel) in the afterburner has occurred. The control unit then allows main afterburner fuel flow to be delivered once a "light-off" has been detected upon pilot-initiated fuel flow.

During afterburning, the detector must maintain an output signal to the control unit which schedules VEN area for the power condition demanded. If the detector output signal is interrupted, the VEN area is restored to the "no-flame" condition. Accordingly, if the detector signal is intermittently interrupted, the VEN will cycle.

From previous tests conducted by GE where flame sensor performance was assessed in engine operation, it was seen that the output pulse rate of certain flame sensors dropped to a low level during certain operating conditions of the engine. When this occurred, the undesirable VEN cycling condition resulted. It was also seen that certain other flame sensors when tested on the engine under similar conditions, were not associated with the VEN cycling condition.

Both flame sensors associated with VEN cycling and those which were not had previously passed the standard bench acceptance test. The test, which had been used historically, involves measurement of flame sensor output pulse rate in response to irradiance from a small air/propane diffusion flame. The test is done with the flame sensor at ambient temperature and again at elevated temperature.

The question was: If all flame sensors tested in the standard bench test delivered a sufficient signal in response to the test propane flame, why should certain of these sensors deliver an insufficient signal during engine operation? Also, could the undesirable VEN cycling condition be a result of one or more contributing factors? Such factors may include variability in the afterburner flame irradiance under certain engine operating conditions and unusually low spectral responsivity of certain flame sensors at elevated temperature.

To answer these questions it was necessary to gain an understanding of three apparent parts to the problem: (1) the relative UV spectral distribution of the engine afterburner flame, (2) the spectral response of the flame sensor as a function of temperature, and (3) the spectral content of the propane flame used historically in bench acceptance testing of flame sensors. Accordingly, Optronic Laboratories was contacted by GE to carry out the spectroradiometric measurements for all three parts of the problem.[1]

This paper describes:

1. The operation of the flame sensors, and
2. The instrumentation, standards and measurement procedures for measuring the spectral responsivities of several sensors at both ambient and elevated temperatures.

The measurements were carried out by Optronic Laboratories at Armtec Industries, Inc. in Manchester, New Hampshire during the periods July 6 to 7, 1988 and July 22, 1988.

2. UV FLAME SENSOR

As is shown in Figure 1, the UV flame sensor or "light-off detector" is mounted directly to the afterburner section of the F404 turbojet engine. Dimensions of the flame sensor are 3.5 inches in diameter by 2.5 inches in height (8.9 cm dia. x 6.4 cm height). Mass of the unit is approximately 1.6 lb. (0.73 kg). The UV flame sensor as shown in Figure 2 contains a proprietary, solar-blind UV detector tube of the gaseous-discharge-type, developed and manufactured by Armtec Industries, Inc. (Armtec is part of the Meggitt Aerospace and Defence Division of Meggitt PLC). This UV detector tube resides within the sealed metal case of the flame sensor unit. Also included within the flame sensor is a UV detector circuit and circuit for pulse output. The UV detector tube views the engine flame through a UV-transmissive window which is mounted in one face of the flame sensor case. Also attached to the flame sensor case is the electrical connector for input power and signal output.

The flame sensor has been designed to operate in the severe environmental conditions associated with the turbojet engine on a high performance attack fighter. Some of the specifications for the flame sensor are listed in Table 1. The operating temperature range for this device is from -65°F to 400°F (-54°C to

204°C). The flame sensor, including the UV detector tube, has been designed to withstand mechanical vibration and impact shock.

The detector consists of a gas-filled tube with parallel metal electrodes. These electrodes act as a closed switch when UV radiation is sensed from the engine's hydrocarbon flame. Ultraviolet radiation from the flame which is incident upon the cathode of the UV detector tube results in photoelectron emission and breakdown of the ionizable gas filling in the detector. A large current flows between the electrodes of the UV detector tube and voltage pulses of positive or negative polarity are fed to the circuit of the engine control unit. It is here where a sufficient number of pulses is integrated into a DC voltage to trigger the control logic that a "light-off" (ignition of fuel) in the afterburner has occurred. The control unit then allows main afterburner fuel flow to be delivered once a "flame-on" signal on the pilot fuel flow has been detected. During afterburning, the detector must maintain an output signal to the control unit which schedules VEN area for the power condition demanded. If the detector output signal is interrupted, i.e., a "flame-off" signal is indicated, the VEN area is reduced. When the signal is reestablished, the VEN area is restored. Accordingly, if the detector signal is intermittently interrupted, the VEN will cycle.

In order to realize the need for spectral response measurements of the flame sensor and the previously reported irradiance measurements of engine flame it is necessary to understand the principles of operation of the UV detector component of the flame sensor. Therefore, a brief description of the UV detector tube and the principles of its operation is presented.

2.1 DEVICE DESCRIPTION - UV DETECTOR TUBE

A picture of the UV detector tube is shown in Figure 3. The tube is 1.65 inches (41.8 mm) in height (including base pins) with a diameter of 1.125 inches (28.6 mm). The tube contains two symmetrical metal electrodes which are parallel to one another. The electrode material used in the detector tube has been selected to ensure that no significant level of response to radiation is seen at wavelengths longer than about 260 nm to 275 nm. As such, the UV detector tube can be considered to be solar-blind. The gas filling of the tube was selected to achieve the desired characteristics for breakdown voltage, conduction current, and recovery time (deionization time).

2.2 PHOTOELECTRIC EMISSION

The operation of the gaseous discharge detector tube is based upon the photoelectric emission effect. When a photon is incident upon the metal cathode it is possible that the energy of the photon can be imparted to a free electron which is near or at the surface of the metal. It is possible for the electron to escape from the surface of the metal only if its kinetic energy exceeds the surface work function of the metal. The equation describing the photoelectric effect is given by

$$E = \frac{hc}{\lambda} - \phi,$$

where E = Energy of the emitted electron
h = Planck's constant
c = Velocity of light
λ = Wavelength of light incident upon metal surface
$\frac{hc}{\lambda}$ = Energy of absorbed photon
ϕ = Surface work function

Thus, photoelectron emission is governed by two factors, the wavelength (λ) of incident radiation, and the energy (ϕ) required to free an electron from the metal surface.

The maximum wavelength at which photoemission can occur is given by

$$\lambda_c = \frac{hc}{\phi}$$

or,

$$\lambda_c(\text{Å}) \simeq \frac{12{,}398}{\phi(\text{e.v.})}$$

If, for example, it is desired to limit response of the detector to ultraviolet radiation having wavelengths shorter than about 300 nm (3000Å), then a cathode material must be selected which has a work function (ϕ) greater than about 4.1 e.v. Numerous materials exist which can satisfy this criterion. The detector will only respond to radiation having wavelength shorter than (λ_c). Detector response is not limited to ultraviolet radiation but includes the x-ray and gamma ray parts of the electromagnetic spectrum as well. Due to the quantum nature of light, the photoemissive wavelength "cut-off" or threshold is a function of the frequency of incident radiation and is not a function of it's irradiance level.

2.3 IONIZATION AND GASEOUS DISCHARGE

Another key principle in the operation of the Armtec UV detector tube is the generation of a measurable current pulse as a consequence of the occurrence of a gaseous discharge between the two parallel metal electrodes. The primary photoelectrons which are ejected from the metal cathode surface as a result of the incidence of UV radiation, are responsible for triggering a gaseous discharge between the electrodes.

A high voltage which is applied across the metal electrodes results in a large electric field between them. The primary photoelectron which has been ejected from the cathode surface becomes accelerated toward the anode. It collides with gas molecules generating an avalanche, i.e., an equal and large number of electrons and ions. The electrons move toward the anode, while the positive gas ions are accelerated toward the cathode. The collision of the ions with the cathode results in the emission from the cathode of an additional number of electrons. These secondary electrons, originating from the single primary photoelectron, result in a multiplication factor in the detector tube. Repetition of this cycle results in current generation between the anode and cathode. The magnitude of this current is prevented from growing continuously by using a current limiting resistor in series with the circuit external to the UV detector tube, as shown in Figure 4. Here, (V_a) is the DC voltage applied to the detector circuit. The resistor (R) limits the current (i) through the circuit to a value determined by the value of (R) and (V_a) as well as by the resistance of the detector tube for a conduction current (i). The voltage across the detector tube during the presence of the gaseous discharge inside the tube is equal to

$$V_m = V_a - (i)(R),$$

and is called the discharge maintenance voltage. The circuit shown in Figure 4 is a "non-quenching" DC circuit since the discharge will persist unless the voltage across the detector tube is reduced to a value smaller than (V_m). The discharge quenching can be achieved by using an AC applied voltage or a DC quenching circuit.

A simple AC circuit for the UV detector tube is shown in Figure 5. When using an AC voltage, the symmetrical electrodes of the UV detector interchange as anode and cathode on alternate half cycles. Also shown in Figure 5 is a representation of AC voltage waveforms for a UV detector tube which is in saturation; that is, the detector is showing a pulse output on each half cycle of excitation. As the voltage rises above the breakdown voltage (V_b), the detector goes into conduction and remains in conduction for time (t_1) until the applied voltage falls below the tube maintenance conduction voltage (V_m). As the phase reverses and the voltage increases, the opposite electrode functions as the cathode and the tube again goes into conduction mode when (V_b) is exceeded. This cycle becomes repeated so that at high frequency a high UV detector pulse rate can be obtained.

An example of a typical DC quenching circuit for use with the UV detector tube is shown in Figure 6. In this simple RC-type circuit quenching of the UV tube discharge occurs because the anode potential is periodically dropped below the tube discharge maintenance voltage (V_m) due to the periodic discharging of the circuit capacitor. In this way, removal of the incident UV radiation results in cessation of the discharge in the tube. When the circuit capacitor discharges through the detector tube, a small current pulse will be measured across resistor (R_2). Monitoring these output pulses as a function of time with an electronic counter provides a means to measure the response of the UV detector tube to incident UV radiation.

2.4 FACTORS GOVERNING UV DETECTOR SENSITIVITY TO UV RADIATION

The UV detector tube is operated within the "normal" glow discharge region of its voltage vs current characteristic curve (region D-E of Figure 7). A current-limiting resistance in the tube circuit is selected such that the conduction current of the detector tube is within the normal glow discharge region. The sensitivity of the detector tube to incident UV radiation is not dependent upon the discharge current, but rather upon the irradiance level and the magnitude of the voltage (V_a) applied to the tube electrodes. Sensitivity is strictly proportional to the UV irradiance level for weak and moderate irradiance levels only. As the irradiance on the detector is increased, the number of discharges or pulses is larger due to the larger number of photoelectrons generated per unit time. When the irradiance level is very large, the detector response is nonlinear and saturation results. When the UV detector is powered with AC excitation, complete saturation is defined as a count rate which is twice the AC frequency. When the UV detector is powered with a DC circuit of the RC-type, the count rate at which saturation occurs depends upon the respective values of the charging resistor and capacitor in this circuit.

UV detector sensitivity is also a function of the applied voltage level (V_a) provided to the tube electrodes. In Figure 7, the breakdown voltage of a UV discharge tube is indicated as (V_b). The overvoltage percentage is defined as $[(V_a - V_b)/V_b] \times 100$. As the overvoltage percentage is made larger by elevating (V_a), the sensitivity of the UV detector tube increases due to the increase in the probability that a primary photoelectron will produce an avalanche of sufficient multiplication to cause gas breakdown.

2.5 UV DETECTOR TUBE SPECTRAL RESPONSE AND SOLAR BLINDNESS

The shape or relative spectral response curve for the detector tube can largely be attributed to two factors, i.e., the surface work function of the detector electrodes, and the UV transmission characteristics of the envelope material for the detector. The electrode work function determines the cut-off or threshold wavelength and is responsible for a decline in spectral response at the long wavelength side of the response maximum. A decline in spectral response associated with the move from the response maximum toward shorter wavelength is due to the decrease in transmission of the detector envelope material. If a fused silica envelope material is used, UV spectral response can extend to a wavelength as short as 160 nm, provided that the UV detector is used in vacuum. When the detector is used with an intervening air path between it and the radiation source, absorption due to molecular oxygen limits the response minimum to about 190 nm to 200 nm.

The Armtec UV detector tube in the GE flame sensor responds to UV radiation from the afterburner flame, but does not respond to visible or infrared radiation emitted from hot engine surfaces.

In addition, the detector shows negligible response to either direct or reflected solar radiation at the earth's surface. Solar spectral irradiance at sea level has been reported to extend to wavelengths as short as 300 nm. In the spectral region from 300 nm to 200 nm (for air mass 1.0, at sea level), nearly complete attenuation of solar radiation occurs due to absorption by atmospheric ozone at high altitude.[2-3] The flame sensor is designed to respond to the UV irradiance from the afterburner flame within a portion of this "solar blind" spectral region. It is also a performance requirement of the flame sensor that it remain unresponsive to solar radiation up to an altitude of 65,000 feet (19.8 km). Of course as altitude increases solar irradiance extends to shorter wavelength owing to the decreased pathlength of solar radiation through atmospheric ozone. Early high altitude solar spectrographic measurements[4] indicate that at an altitude of 100,000 feet (30.4 km) solar irradiance can extend to wavelengths as short as 275 nm, a region near the long wavelength threshold of the flame sensor. However, up to this altitude the flame sensor should show no significant response to solar radiation.

3. INSTRUMENTATION

3.1 SPECTRORADIOMETRIC INSTRUMENTATION

Spectral responsivity measurements on the flame sensors were made using an Optronic Laboratories Model 740A/D Optical Radiation Measurement System/Double Monochromator Option (Figure 8). The system was optimized for measurements over the 200 to 300 nm wavelength region.

A system employing a double monochromator for the optical dispersing mechanism was considered essential in order to minimize the effect of stray light. An optical layout of the monochromator is shown in Figure 9. It is a rugged, research grade double-grating monochromator intended for laboratory applications where high-intensity and extremely high-purity radiation is needed. Outstanding attributes of the monochromator are its fast optical speed (f/4), grating efficiencies at blaze wavelengths of greater than 70%, and an extremely low scattered light level.

The optical path of the monochromator is basically a Czerny-Turner configuration with two concave mirrors and a plane grating arranged as the letter "M". Behind the entrance and exit slits are 45° mirrors which provide an in-line path for source and output. The double monochromator is essentially two in-line single monochromators. This classic design in widely used because of its aberration correcting properties.

The two 50 x 50 mm gratings blazed at 250 nm and having 1200 grooves/mm were selected in order to optimize the monochromator performance over the 200-300 nm wavelength region. The dispersion factor for the monochromator was 2 nm/mm. Five sets of fixed slits having widths of 0.25, 0.5, 1.25, 2.5, and 5 mm and producing half bandwidths of 0.5, 1.0, 2.5, 5, and 10 nm were available for the measurements. Specifications for the double monochromator are given below.

Wavelength Range	200 to 500 nm
Dispersion	2 nm/mm
Wavelength Accuracy	±0.2 nm
Wavelength Precision	±0.1 nm
Bandwidth	0.5, 1, 2.5, 5, and 10 nm
Stray Light	Less than 10^{-6}
Size	53 x 46 x 25 cm
Weight	27 kg

The Optronic Laboratories Model 740-1C Automatic Wavelength Drive-Filter Wheel Controller was used to control the wavelength and the second order blocking filters. The unit consists of:

1. A stepper motor drive
2. A high-accuracy, bi-directional optical shaft encoder
3. An automatic second order blocking filter wheel
4. A control chassis for the wavelength drive electronics

The stepper motor, optical shaft encoder, and blocking filter systems are located inside the monochromator while the controller is a separate module. The controller provides for manual pushbutton control or remote computer control of the wavelength scanning of the monochromator. It provides the interface function between the double monochromator and computer. The optical shaft encoder is connected to the wavelength drive shaft and produces accurate data which is digitally displayed in the control chassis. The resolution of the digital wavelength display is 0.1 nm. BCD wavelength information is available for controlling the wavelength drive automatically via a remote computer. The motorized filter wheel containing the proper second order blocking filters is mounted just inside the entrance port of the monochromator. A wavelength signal generated by a precision 10-turn potentiometer is used to produce a drive coded signal for the filter wheel motor.

The source unit consisted of an Optronic Laboratories Model 740-20D/UV Dual High Intensity Source Attachment. This attachment consists of a compact 150 watt quartz halogen lamp and 50 watt deuterium lamp. An optical schematic of the attachment is shown in Figure 10. The sources are aligned and pre-focused and can be imaged onto the entrance slit of the double monochromator through the use of a manual beam switching mirror. The deuterium lamp, which was used exclusively for these measurements, is a high intensity UV source with a peak output at about 200 nm. In addition, the arc produces a continual (or line-free emission) spectral output over the 200 to 400 nm wavelength region. An Optronic Laboratories Model 45D Precision DC Constant Current Source was used to power the deuterium lamp. The uncertainty in the current generated by the Model 45D is ±0.1%.

An Optronic Laboratories Model 740-72 Quartz Lens Collimator was attached to the exit port of the double monochromator. An optical schematic of the Model 740-72 is shown in Figure 11. This attachment uses a 3-inch focal length, fused silica lens to semi-collimate the monochromatic beam exiting the monochromator. A 1 cm^2 aperture was placed at the end of the collimating tube. This provided a well-defined, uniform beam for irradiating both the standard detector and the flame sensor with the same monochromatic flux.

The calibrated detector consisted of an Optronic Laboratories Model 730-5C UV-enhanced, silicon detector. The detector attached directly to the end of the collimating tube via a precision, machined coupling sleeve.

An Optronic Laboratories Mode 730A Autoranging Radiometer/Photometer was used to measure the current generated by the calibrated detector. The Model 730A has full scale ranges from 10^{-4} to 10^{-10} amperes and a resolution of 10^{-13} amperes. The linearity of the full range is ±1% ±1 digit. The unit has BCD data and digital control lines for computerized operation.

Both wavelength and detector signals were transmitted to a PC using the Optronic Laboratories Model 740-410 BCD Interface Cable and Card. The Model 740-425 Detector Spectral Response Software Package enabled the PC to control the entire measurement process and to obtain data on a real time basis.

3.2 CONTROLLED-TEMPERATURE OVEN, FLAME SENSOR POWER SUPPLY, AND PULSE COUNTING ELECTRONICS

Spectral responsivity measurements of flame sensors were carried out at 70°F and at 400°F. For these tests, each flame sensor was placed inside of a Delta (Model 5900FL) controlled-temperature oven. The oven was resistance-heated and liquid nitrogen-cooled such that a setpoint temperature accuracy of ±0.2°F was achieved. The heating and cooling profile was controlled by a personal computer to be the same for each flame sensor tested.

During spectral responsivity measurements, the flame sensor was connected to a General Electric Flame Sensor Test Set which provided input power to the flame sensor. The Test Set also converted the raw pulse output of the flame sensor into a conditioned pulse output signal (in counts per second).

When the flame sensor (inside the oven) was subjected to UV radiation from the source-module/double-monochromator/quartz-lens-collimator unit (located outside of the oven), a pulse output resulted. For each 2 nm wavelength interval scanned, the average of six consecutive, conditioned response values (in counts per second) from the flame sensor was entered into the computer system of the optical measurement system.

4. STANDARDS AND UNCERTAINTIES

The monochromatic flux incident upon the flame sensor was determined by placing a calibrated, UV-enhanced detector directly against the 1 cm^2 aperture at the end of the Quartz Lens Collimator. This detector was calibrated for amps/watt over the wavelength range of 200 to 260 nm by the Far UV Physics Group at NIST.[5] The uncertainty in the reported spectral response values is ±5%. For the region above 250 nm, the calibration is based on the NIST Photodetector Spectral Response Calibration Transfer Package.[6] The reported uncertainty in the NIST scale over the wavelength range of 250 to 300 nm is 6.0%. The transfer uncertainty to the Optronic Laboratories Model 730-5C calibrated detector is estimated at ±1%. Accordingly, the uncertainty in the monochromatic flux at the end of the Quartz Lens Collimator relative to the NIST scale is estimated to be less than ±2% over the 200 to 300 nm wavelength range.

5. EXPERIMENTAL SET-UP AND MEASUREMENT PROCEDURE

The experimental set-up when determining the monochromatic flux using the standard detector is shown in Figure 12. The Model 740-20D/UV light source was attached to the entrance port of the double monochromator. The Quartz Lens Collimator formed a uniform, semi-collimated, monochromatic beam. The calibrated detector was positioned against the 1 cm^2 aperture.

The signal generated by the detector in amperes was amplified and displayed by the Model 730A Autoranging Radiometer. The setting of wavelength and display of wavelength was controlled by the Model 740-1C Automatic Wavelength Drive-Filter Wheel Controller Unit. BCD signals of both detector output and wavelength were fed into a PC for automatic operation.

The PC controlled the wavelength scanning, printed out the correct wavelength and detector signal, and computed the monochromatic flux. Figure 13 shows a typical monochromatic flux output curve over the measurement range of 200-300 nm.

Once the monochromatic flux was determined, the calibrated detector was removed and the optical portion of the measurement system (source-module/double-monochromator/quartz-lens-collimator) was positioned such that the known monochromatic flux was incident on the flame sensor which was located in the oven.

The standard computer software program for measuring spectral response of detectors was modified for the testing of the flame sensors in order to accommodate the flame sensor's signal processing electronics. The flame sensor's output was measured in counts per second.

The measurement procedure was as follows:

1) Measure monochromatic flux by placing calibrated detector at measurement plane.

2) Position optical measurement system such that the flame sensor (while in the oven) was at the measurement plane.

3) Automatically scan over desired wavelength range and interval pausing at each wavelength of interest and noting the output (counts per second) of the flame sensor.

4) Repeat Step 3 above after the flame sensor had attained a temperature of 400°F for 30 minutes and 400°F for 60 minutes.

The pertinent optical parameters for the measurements were as follows:

Wavelength Range	200 to 260 nm
Half Bandwidth	2 nm
Wavelength Interval	2 nm

6. RESULTS

A total of seven flame sensors were completely tested over the entire cycle. Tables 2 to 4 give values of spectral responsivity for three of the flame sensors which are representative of the group. Corresponding spectral response curves are given in Figures 14 to 16. All values are given in counts/sec per watt as a function of wavelength.

In comparison of Figures 14 to 15, it can be seen that the corresponding flame sensors showed a significant loss in spectral response at all wavelengths at a temperature of 400°F as compared to the case where the flame sensors were at room temperature (T = 70°F). The flame sensor with spectral response shown in Figure 16, however, does not show a significant decrease in spectral response at 400°F as compared with its response at 70°F.

These same three flame sensors had been previously tested by General Electric Company on an F404 aircraft engine under several different engine operating conditions to determine whether the undesirable VEN cycling problem was associated with the flame sensors. Their tests had shown that two of the flame sensors (serial number 51618 and 53090) were associated with VEN cycling, but that one flame sensor (serial number 50835) was not.

Good correlation was seen between the large decrease in the spectral response of flame sensors 51618 and 53090 at elevated temperature and the VEN cycling condition which was experienced during engine testing of these two flame sensors.

Previous measurements[1] of the spectral distribution of the F404 afterburner flame had shown a variability in the spectral irradiance of the flame vs wavelength for different engine operating conditions. These measurements also showed that repeated scans on the spectral output of the afterburner for the same operation conditions varied from 2% to 15%.

In view of the results from these previous measurements, together with the results from the present study on the spectral response of flame sensors, the occurrence of the VEN cycling condition appears to be due to a combination of two effects:

1. The Fact that certain flame sensors showed much lower spectral responsivity at elevated temperature than would normally be the case for these devices, and

2. Reduced spectral radiance of the afterburner flame occurred under certain operating conditions of the engine.

This combination of effects apparently resulted in a flame sensor output signal which was below the minimum acceptable threshold to maintain a "flame-on" signal during operation of the afterburner.

These spectroradiometric measurements of engine flame and spectral responsivity measurements of flame sensors were useful not only in isolating the causes of the VEN cycling problem, but were also helpful in finding a solution to the problem. Changes were subsequently made in the acceptance test procedure and test criteria for flame sensors which guaranteed a sufficiently high responsivity value at elevated temperature which could compensate for variability of the afterburner flame spectral irradiance.

7. SUMMARY

The spectral responsivity measurements of UV flame sensors coupled with previous spectroradiometric measurements of the ultraviolet output of a GE F404 aircraft engine were instrumental in identification of the causes of the VEN cycling problem. Low spectral responsivity of certain, selected flame sensors at elevated temperature, coupled with variability in the spectral irradiance of afterburner flame were seen as probable causes. Review of the spectral measurement also assisted in finding a solution to the problem which was to modify the acceptance test and test criteria for flame sensors such that a higher responsivity level was guaranteed at elevated temperature than historically had been the case. This guaranteed a sufficiently high flame sensor output signal level despite variability in afterburner flame irradiance associated with differences in engine operating conditions.

8. ACKNOWLEDGEMENTS

The authors wish to express their appreciation to Bill Santspree, Bill Gorlitz, and Jonathan Plimpton for assisting in the overall measurement program and to Theresa Schehr for her word processing efforts.

9. REFERENCES

1. W.E. Schneider and G.H. Spaberg, "UV Spectroradiometric Output of an F404 Turbojet Aircraft Engine," Conference 1109, paper #18, SPIE 1989 Technical Symposia on Aerospace Sensing, March 28, 1989. (to be published in SPIE Proceedings, Vol. 1109).

2. R.E. Huffman, "Atmospheric Emission and Absorption of Ultraviolet Radiation," in Handbook of Geophysics and the Space Environment, A.S. Jursa, ed., P. 22-4, 1985.

3. A.T. Mecherikunnel and J.C. Richmond, "Spectral Distribution of Solar Radiation," NASA Technical Memorandum 82021, September, 1980.

4. W.A. Baum, et. al. Phys. Rev. 70, 781 (1946).

5. R.P. Madden, "UV and VUV Radiometry at NIST," CORM '89 International Conference on Optical Radiation Measurements, May 17-19, 1989.

6. E.F. Zalewski, NBS Measurement Series: "The NBS Photodetector Spectral Response Calibration Transfer Program," NBS Special Publication 250-17, March 1988.

TABLE 1

GE Flame Sensor Specifications

Environmental Conditions

Operating Temperature	-65°F to +400°F
Altitude	65,000 Feet
Pressure	60 PSIG
Explosion Proof	MIL-STD-810, Method 511-1
Humidity	95% RH @ 75°C (167°F)
Vibration	5 to 2000 Hz, 20 G
Impact Shock	30G, 10 Milliseconds

Physical Characteristics

Weight	Approximately 1.6 lbs.
Size	3.5" Dia. x 2.5" Height
Mounting	3-Hole Bolt Pattern

Performance

Input	AC Driven
Frequency	2000 to 4000 Hz
Output Signal, Flame On	±10 V to 37 V (Peak)
Output Signal, Flame Off	0 Volts
Spectral Response	1900 to 2600 Angstroms No response above 2900 Angstroms; i.e. sun-light
Dielectric Withstanding Voltage (RMS) @ 60 Hz	1500 V
Insulation Resistance	20 megohms @ 500 VDC

TABLE 2

Spectral Response of LOD # 51618 (Linear)

Wavelength (nm)	Spectral Response (counts/sec per watt) * @ 70°F	@ 400°F (30 min)	@ 400°F (60 min)
200	2.92E+11	6.71E+10	6.16E+10
202	2.88E+11	5.58E+10	4.62E+10
204	2.66E+11	4.83E+10	4.02E+10
206	2.37E+11	4.16E+10	3.28E+10
208	2.11E+11	3.53E+10	2.89E+10
210	1.85E+11	2.88E+10	2.29E+10
212	1.65E+11	2.36E+10	1.82E+10
214	1.46E+11	1.70E+10	1.33E+10
216	1.37E+11	1.17E+10	1.02E+10
218	1.25E+11	8.71E+09	6.44E+09
220	1.18E+11	5.00E+09	4.68E+09
222	1.11E+11	3.48E+09	2.99E+09
224	1.02E+11	2.35E+09	1.71E+09
226	9.05E+10	1.19E+09	1.08E+09
228	8.11E+10	5.70E+08	6.22E+08
230	6.86E+10	3.32E+08	3.79E+08
232	5.58E+10	1.40E+08	2.64E+08
234	4.46E+10	8.30E+07	1.24E+08
236	3.51E+10	4.01E+07	8.02E+07
238	2.67E+10	2.40E+07	3.96E+07
240	1.85E+10	1.50E+07	2.60E+07
242	1.21E+10	0.00E+00	1.20E+07
244	7.23E+09	0.00E+00	0.00E+00
246	3.92E+09	0.00E+00	0.00E+00
248	1.26E+09	0.00E+00	0.00E+00
250	4.09E+08	0.00E+00	0.00E+00
252	2.47E+08	0.00E+00	0.00E+00
254	1.25E+08	0.00E+00	0.00E+00
256	8.42E+07	0.00E+00	0.00E+00
258	4.27E+07	0.00E+00	0.00E+00
260	0.00E+00	0.00E+00	0.00E+00

* Central 1 cm^2 portion of LOD uniformly irradiated.
LOD signal level below 4000 counts/sec for all wavelengths.

TABLE 3
Spectral Response of LOD # 53090
(Linear)

Wavelength (nm)	Spectral Response (counts/sec per watt) * @ 70°F	@ 400°F (30 min)	@ 400°F (60 min)
200	6.53E+11	2.07E+11	1.35E+11
202	5.87E+11	1.81E+11	1.26E+11
204	5.28E+11	1.59E+11	1.15E+11
206	4.63E+11	1.52E+11	9.93E+10
208	4.10E+11	1.34E+11	8.89E+10
210	3.77E+11	1.17E+11	7.57E+10
212	3.35E+11	1.00E+11	6.36E+10
214	3.01E+11	8.72E+10	5.50E+10
216	2.71E+11	7.56E+10	4.65E+10
218	2.44E+11	6.61E+10	3.90E+10
220	2.20E+11	5.74E+10	3.22E+10
222	1.98E+11	4.82E+10	2.79E+10
224	1.75E+11	4.00E+10	2.19E+10
226	1.57E+11	3.24E+10	1.82E+10
228	1.35E+11	2.52E+10	1.31E+10
230	1.14E+11	1.87E+10	9.87E+09
232	9.48E+10	1.31E+10	6.25E+09
234	7.59E+10	8.40E+09	3.97E+09
236	6.06E+10	5.24E+09	2.35E+09
238	4.67E+10	2.87E+09	9.57E+08
240	3.35E+10	1.28E+09	2.25E+08
242	2.25E+10	4.22E+08	3.24E+07
244	1.34E+10	6.56E+07	0.00E+00
246	6.59E+09	3.31E+07	0.00E+00
248	2.74E+09	0.00E+00	0.00E+00
250	7.08E+08	0.00E+00	0.00E+00
252	2.40E+08	0.00E+00	0.00E+00
254	6.92E+07	0.00E+00	0.00E+00
256	2.30E+07	0.00E+00	0.00E+00
258	0.00E+00	0.00E+00	0.00E+00
260	0.00E+00	0.00E+00	0.00E+00

TABLE 4
Spectral Response of LOD # 50835
(Linear)

Wavelength (nm)	Spectral Response (counts/sec per watt) * @ 70°F	@ 400°F (30 min)	@ 400°F (60 min)
200	4.35E+11	3.75E+11	2.95E+11
202	4.18E+11	4.02E+11	3.19E+11
204	4.06E+11	4.04E+11	3.46E+11
206	3.63E+11	3.88E+11	3.37E+11
208	3.54E+11	3.73E+11	3.37E+11
210	3.42E+11	3.63E+11	3.09E+11
212	3.27E+11	3.48E+11	2.85E+11
214	3.10E+11	3.24E+11	2.74E+11
216	2.89E+11	3.12E+11	2.64E+11
218	2.70E+11	2.88E+11	2.53E+11
220	2.48E+11	2.75E+11	2.41E+11
222	2.30E+11	2.51E+11	2.31E+11
224	2.08E+11	2.38E+11	2.15E+11
226	1.84E+11	2.15E+11	1.93E+11
228	1.59E+11	1.75E+11	1.74E+11
230	1.38E+11	1.48E+11	1.49E+11
232	1.14E+11	1.23E+11	1.24E+11
234	9.04E+10	1.00E+11	1.07E+11
236	7.32E+10	8.20E+10	8.45E+10
238	5.67E+10	6.33E+10	6.75E+10
240	4.13E+10	4.86E+10	5.22E+10
242	2.92E+10	3.57E+10	3.68E+10
244	1.88E+10	2.32E+10	2.43E+10
246	1.07E+10	1.40E+10	1.53E+10
248	4.60E+09	7.60E+09	7.79E+09
250	1.70E+09	3.26E+09	3.69E+09
252	4.28E+08	1.52E+09	1.57E+09
254	1.44E+08	5.30E+08	7.22E+08
256	4.87E+07	2.92E+08	2.43E+08
258	0.00E+00	9.86E+07	1.48E+08
260	0.00E+00	4.99E+07	4.99E+07

* Central 1 cm^2 portion of LOD uniformly irradiated.
LOD signal level below 4000 counts/sec for all wavelengths.

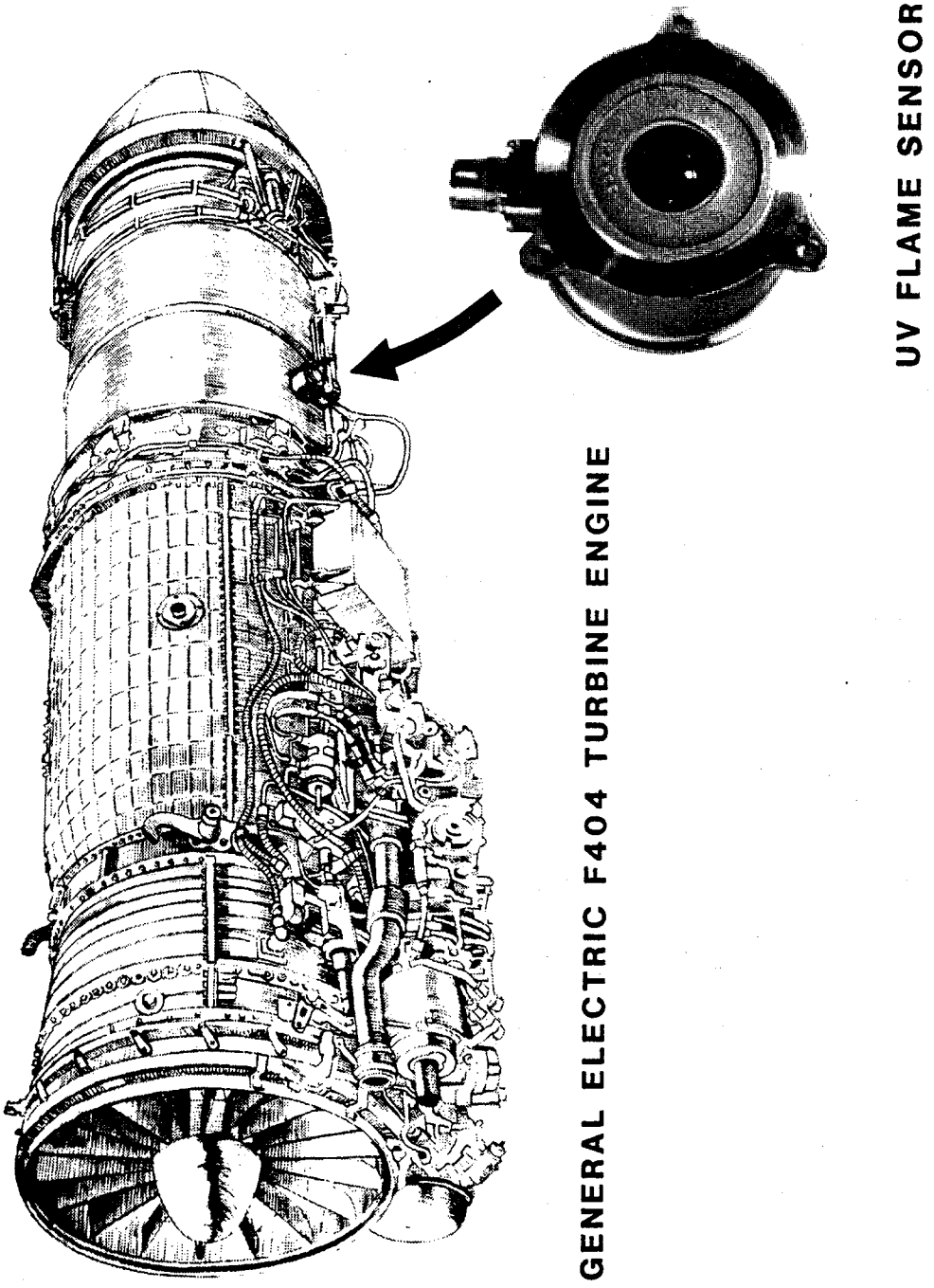

Figure 1. UV Flame Sensor Location on F404 Turbine Engine

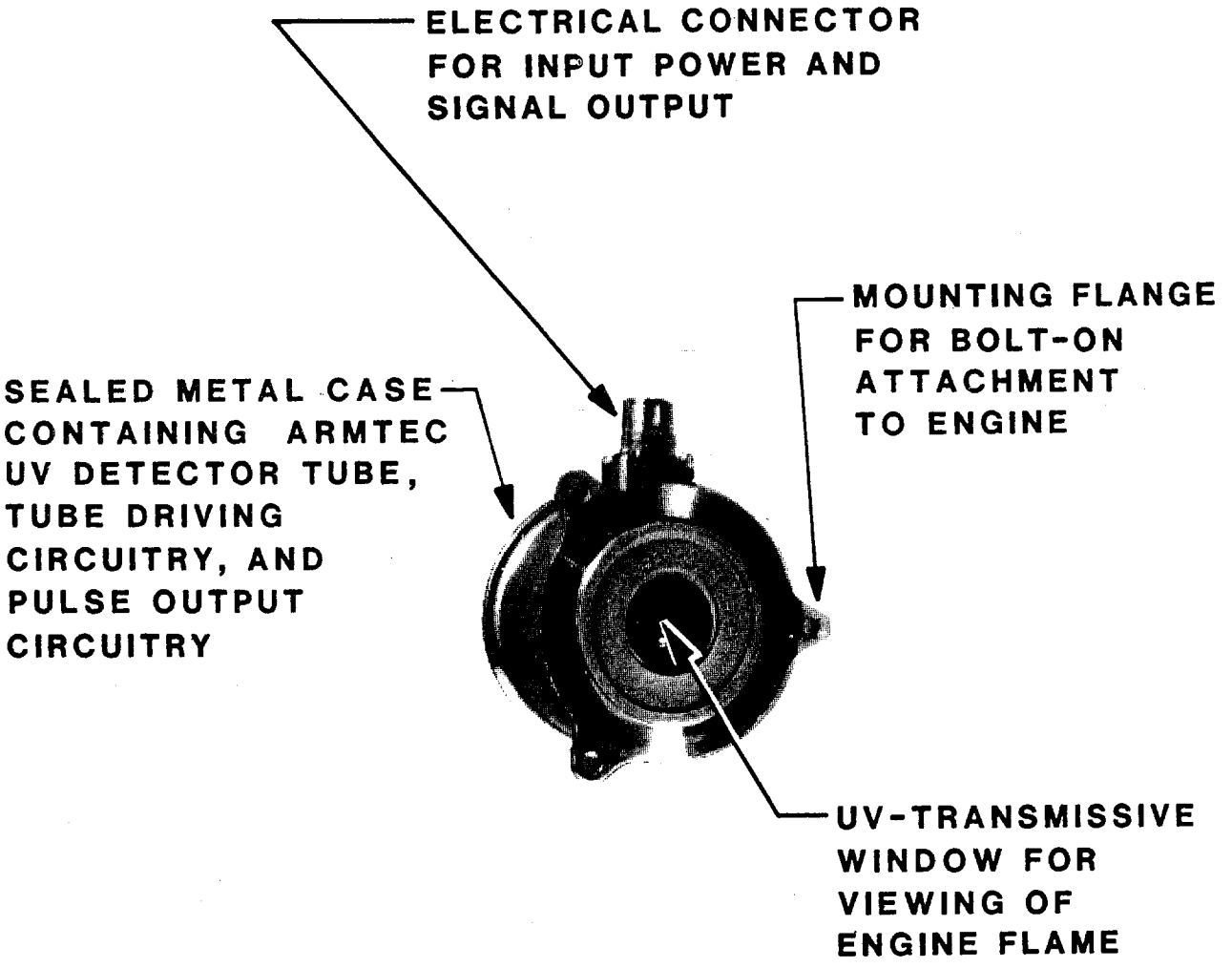

Figure 2. General Electric UV Flame Sensor

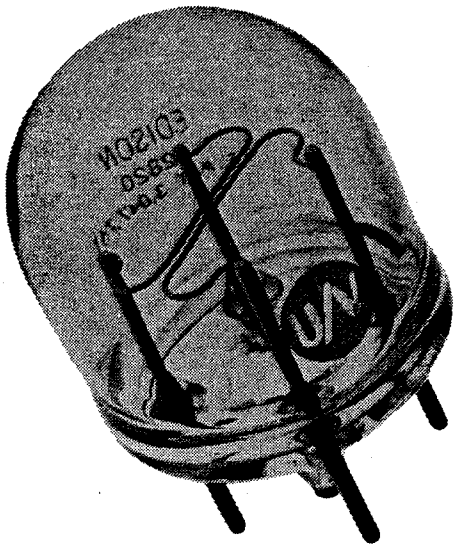

Figure 3. Armtec UV Detector Tube

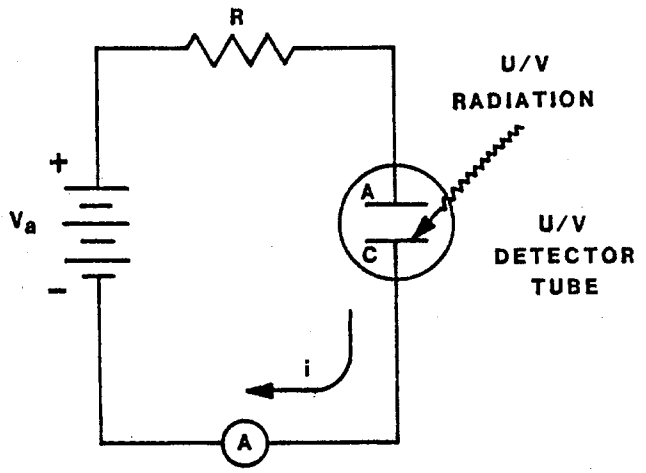

Figure 4. Simple Non-Quenching DC Circuit for U/V Detector Tube

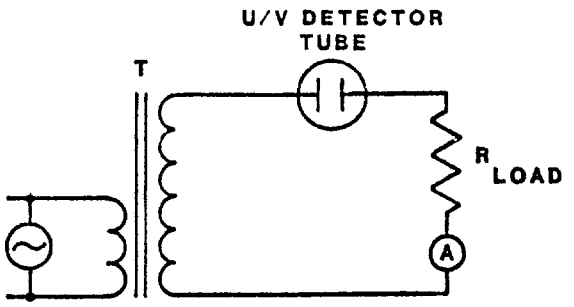

SIMPLE AC QUENCHING CIRCUIT FOR U/V DETECTOR TUBE

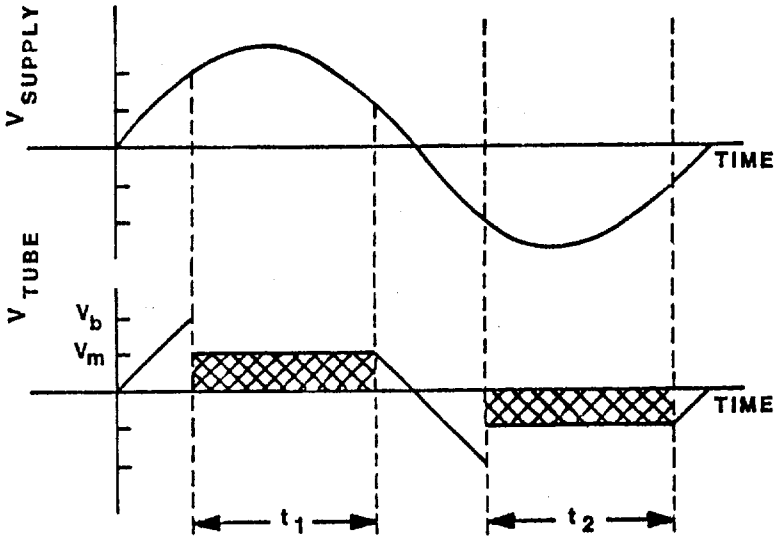

Figure 5. AC Waveforms for Supply and U/V Detector at Saturation

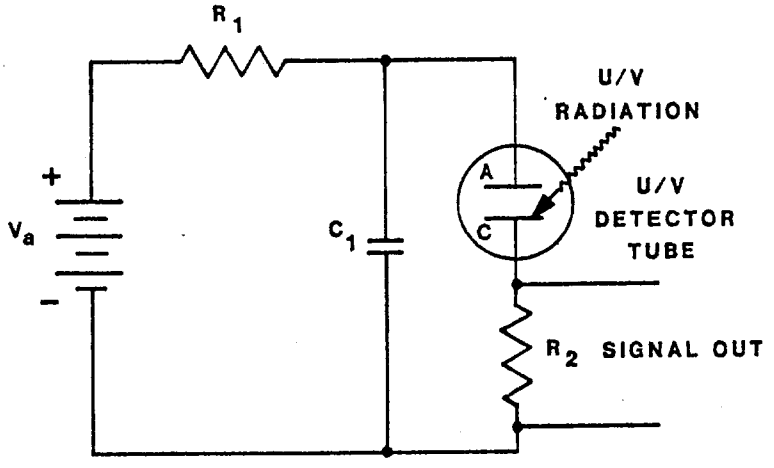

Figure 6. Simple DC Quenching Circuit for U/V Detector Tube

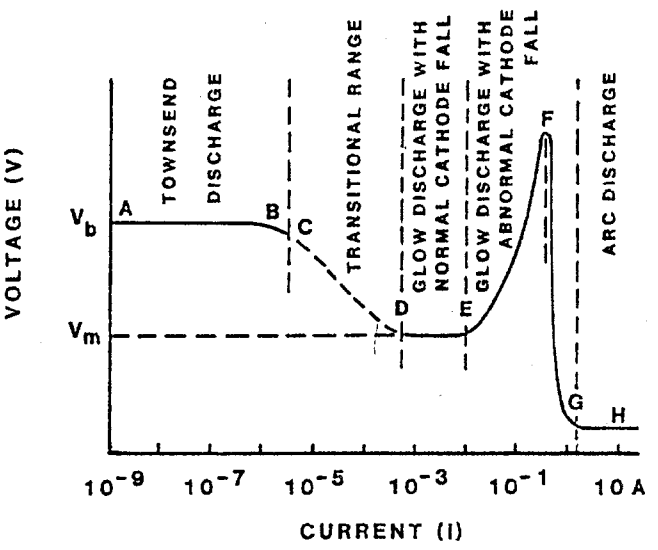

Figure 7. Glow Discharge

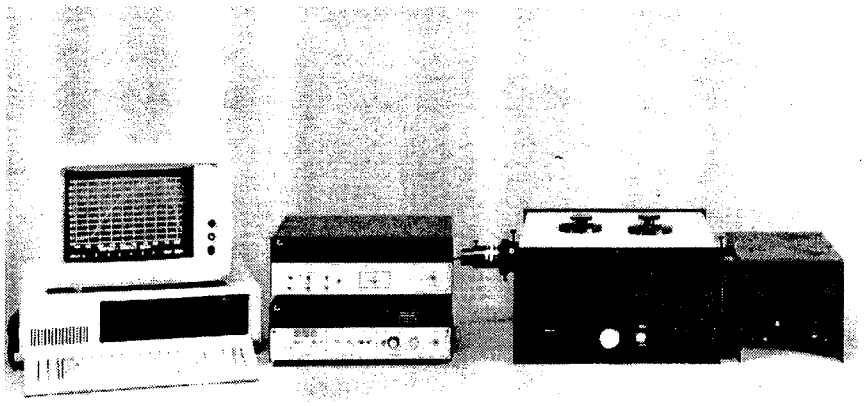

Figure 8. Model 740A/D Optical Radiation Measurement System

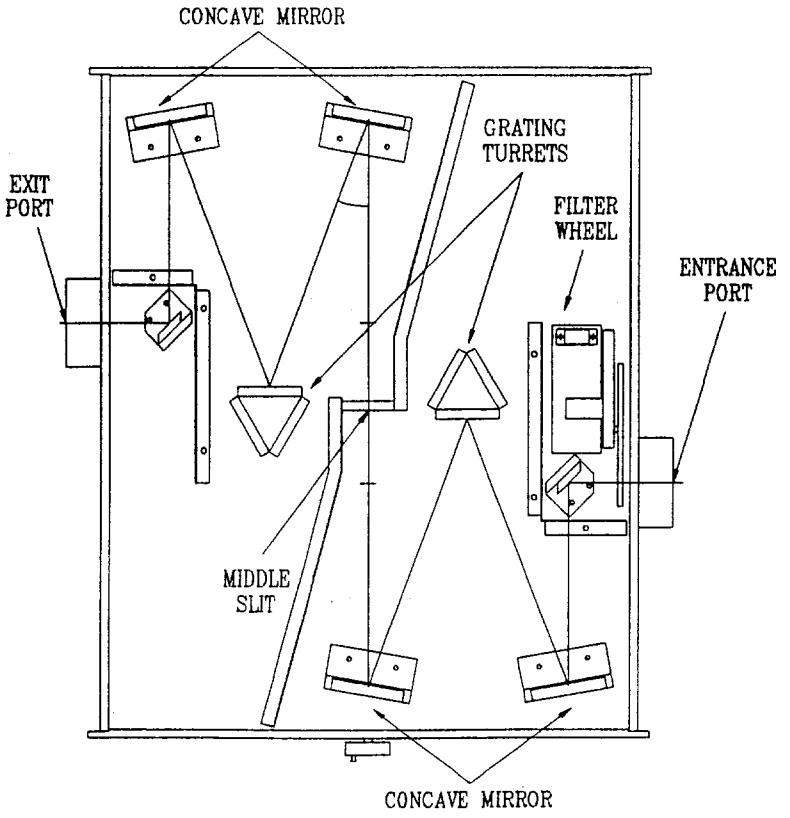

Figure 9. Double Monochromator

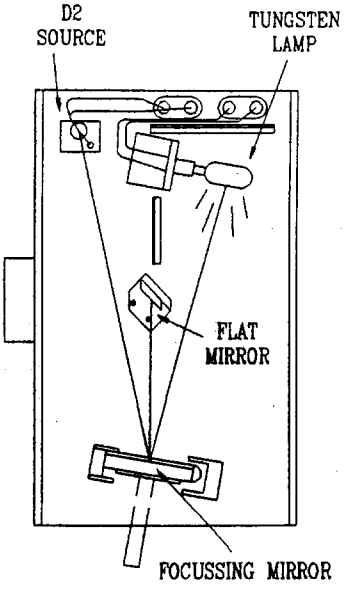

Figure 10. Dual Source Module

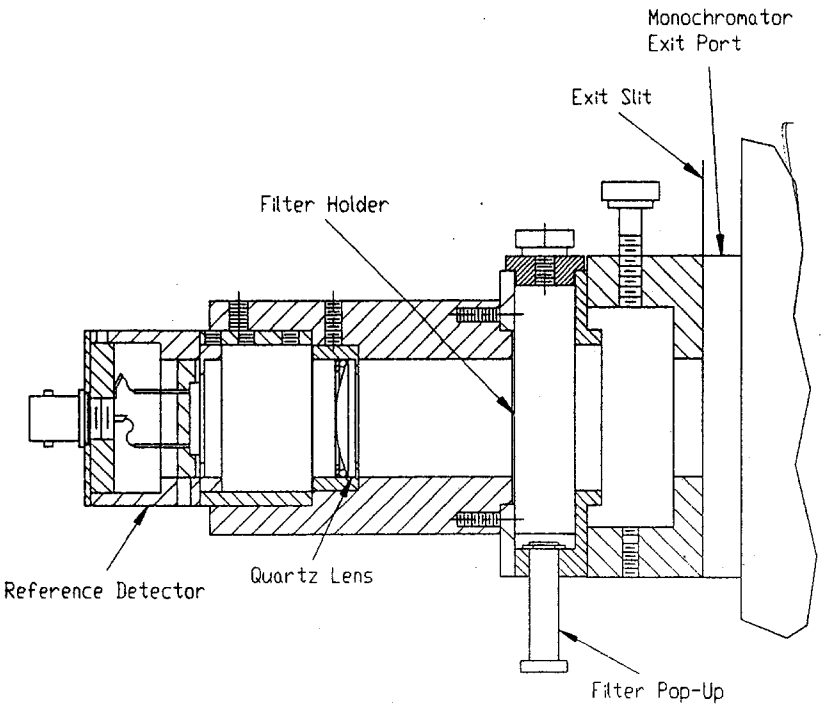

Figure 11. Quartz Lens Collimator

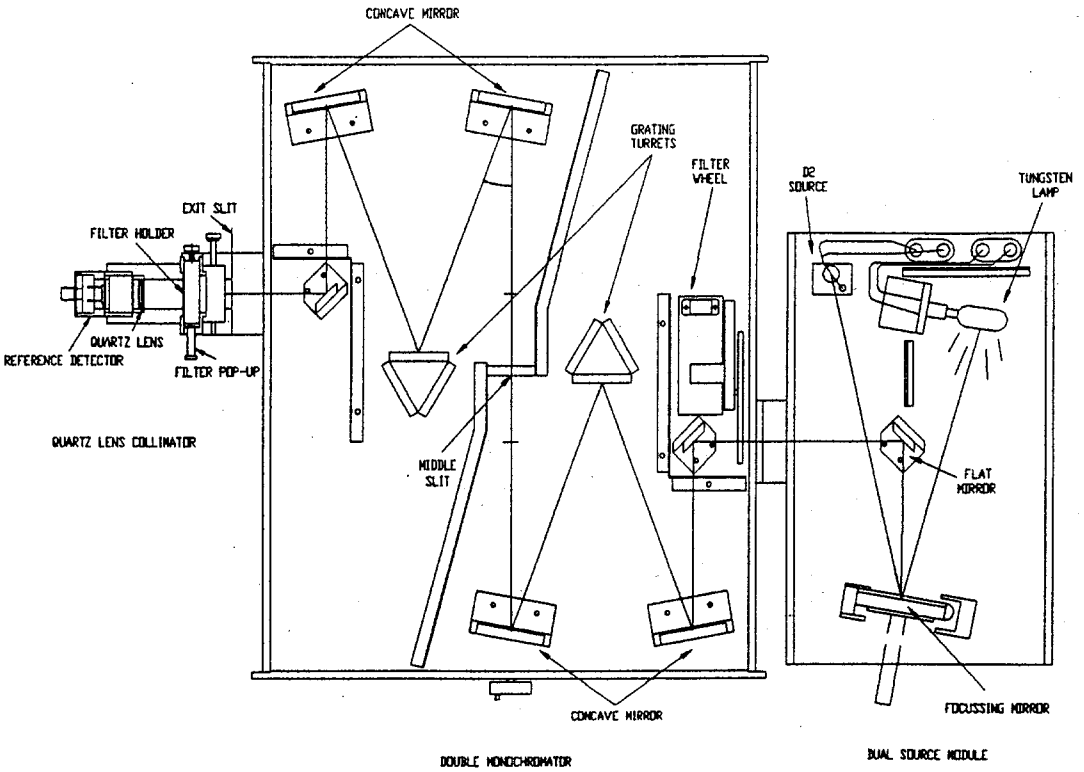

Figure 12. Optical Schematic of Model 740A/D Optical Radiation Measurement System

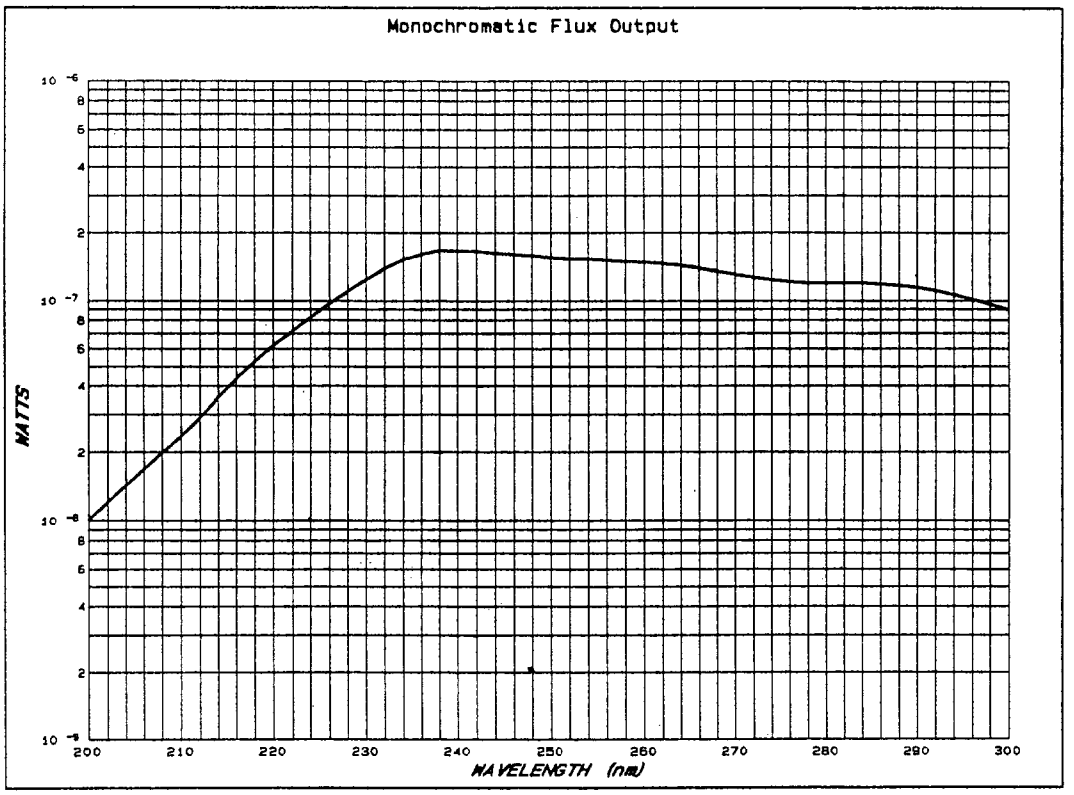

Figure 13. Typical Monochromatic Flux Output

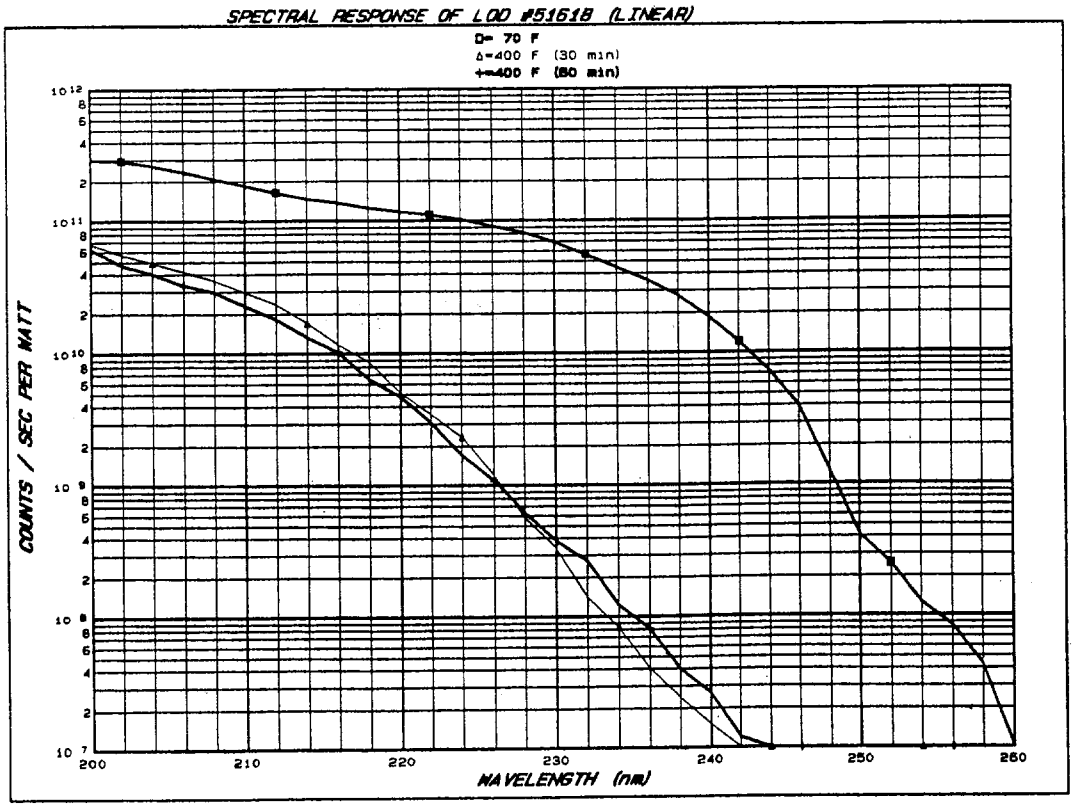

Figure 14. Spectral Response of LOD #51618 (Linear)

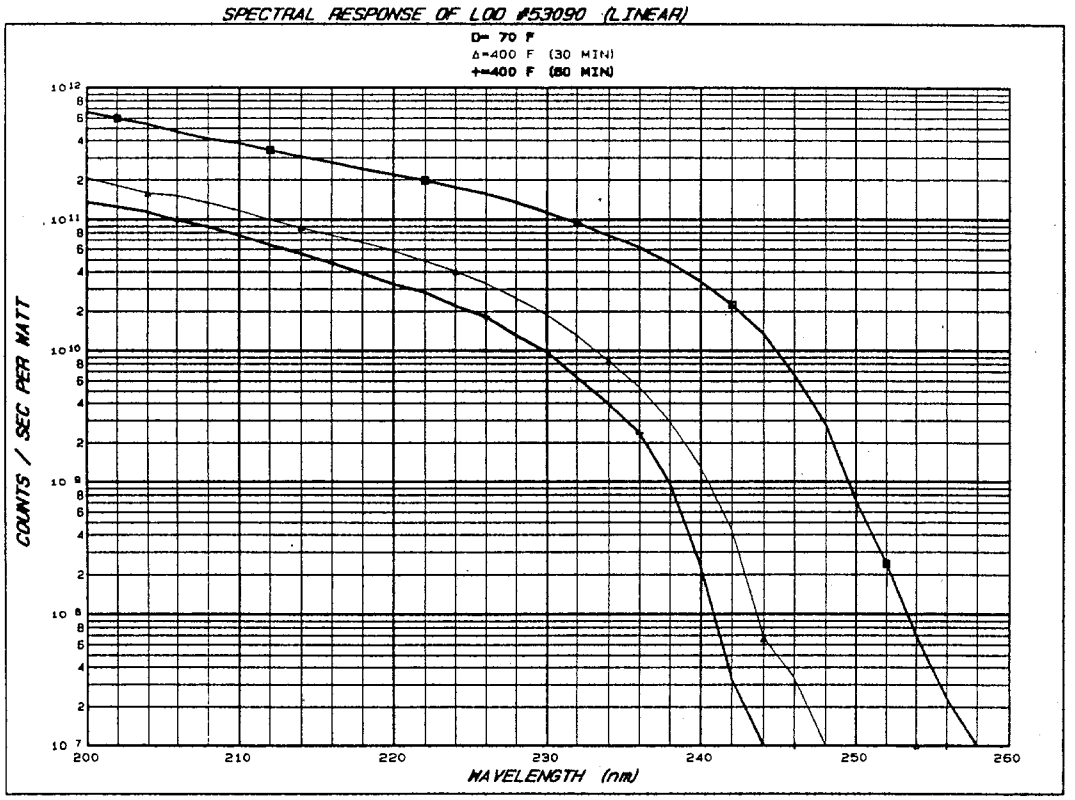

Figure 15. Spectral Response of LOD #53090 (Linear)

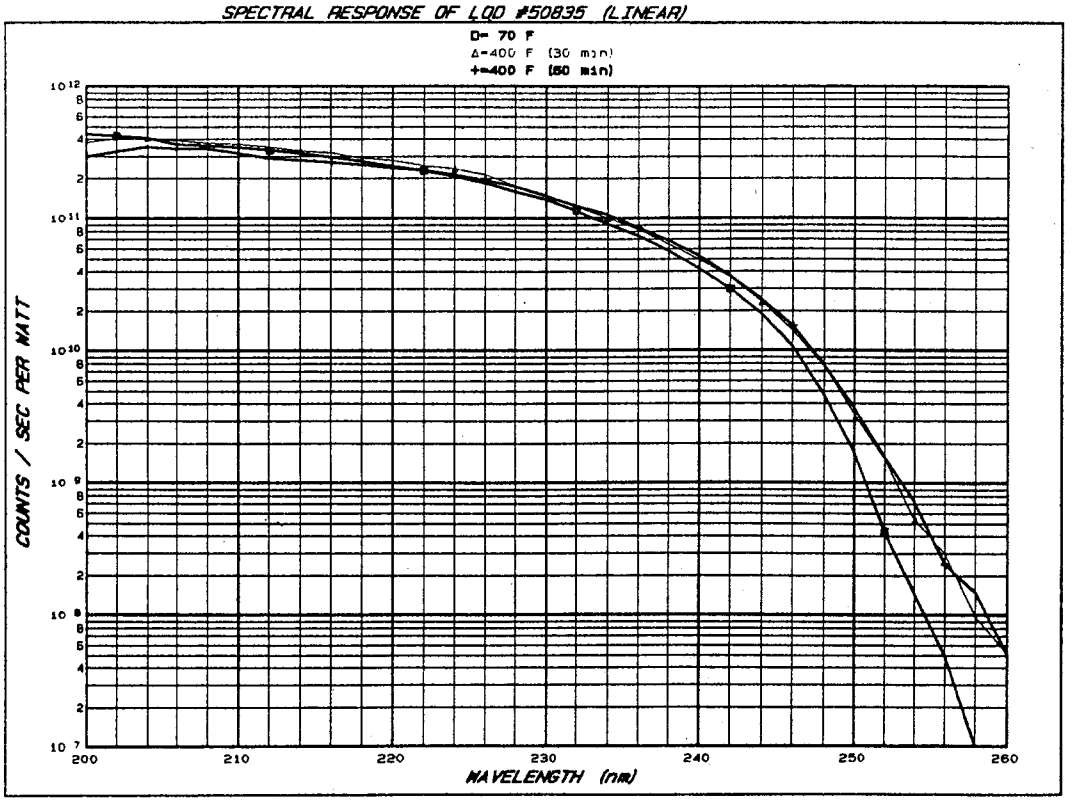

Figure 16. Spectral Response of LOD #50835 (Linear)